

Chapter 2

Reversible Oxygen-Binding to Simple and Planar Cobaltporphyrins Combined with Polymeric Imidazole.

2.1 Introduction

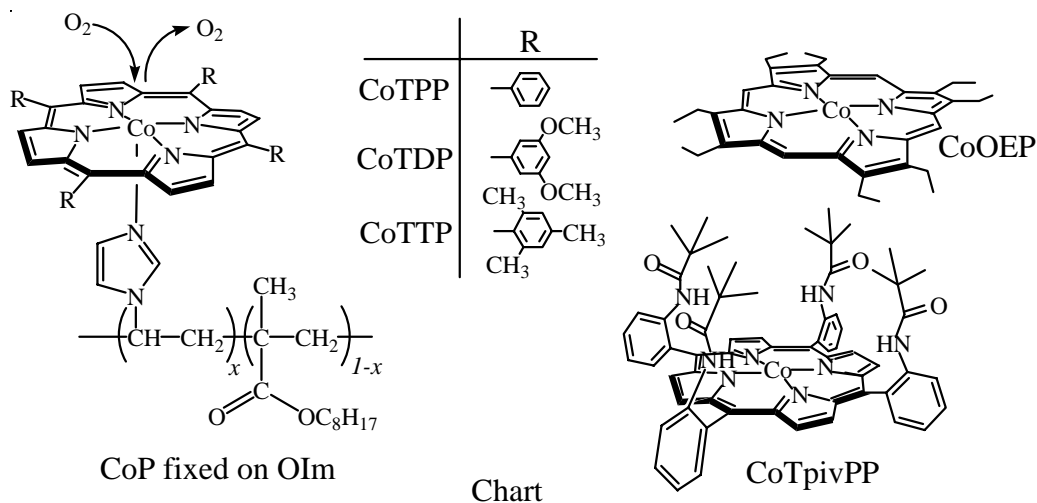
Much research has been devoted to mimicing oxygen carriers like hemoglobin by synthesizing modified metalloporphyrins from the middle of the 70's.¹⁻³ A typical example is the iron- or cobalt-picketfence porphyrin or *-meso- $\alpha,\alpha,\alpha,\alpha$ -tetrakis(*o*-pivalamidophenyl)porphyrinatocobalt* (CoTpivPP, Chart)⁴ which has four pivalamido groups on one side of the porphyrin plane to provide a cavity for oxygen-binding and the other side is available for complexing with a nitrogenous ligand such as imidazole to improve the oxygen-binding affinity. On the other hand, while a simple or planar cobaltporphyrin without any cavity structure (CoP) forms the 5-coordinated complex with imidazole in a solution at room temperature, the CoP complex cannot bind oxygen and is gradually oxidized from cobalt(II) to (III) upon exposure to air.

Ibers et al.⁵⁻⁷ reported in the early 70's that even simple CoPs with a nitrogenous ligand reversibly form their oxygen adducts at low temperature (-5--40°C) in an organic solvent and have described the formation constant of the oxygen adducts, their temperature dependency, and effects of the ligands. The authors have also reported the oxygen-binding by the cobalt-protoporphyrin IX dimethyl ester complex of poly(4-vinylpyridine-*co*-styrene) in a cooled toluene solution and studied the polymer complex as one of the hemoglobin models at that time.^{8,9} This chapter describes the reversible oxygen-binding to cobalt-tetraphenylporphyrin (CoTPP) and its derivatives and cobalt-octaethylporphyrin (CoOEP) combined with the copolymer of vinylimidazole and octyl methacrylate (OIm) in a cooled dichloromethane solution.

2.2 Experimental

2.2.1 Materials

Cobalt-5,10,15,20-tetraphenylporphyrin and cobalt-2,3,7,8,12,13,17,18-octaethylporphyrin were purchased from Aldrich Co., Ltd and used as received while cobalt-*meso*-tetrakis(3,5-dimethoxyphenyl)porphyrin (CoTDP), cobalt-*meso*-tetrakis(2,4,6-trimethylphenyl)porphyrin (CoTTP) were synthesized from *meso*-tetrakis(3,5-dimethoxyphenyl)porphyrin, and *meso*-tetrakis(2,4,6-trimethylphenyl)porphyrin



after insertion of cobalt metal with cobalt acetate using a literature method.¹⁰ Poly(1-vinylimidazole-*co*-octyl methacrylate)(OIm in Scheme) was prepared by radical polymerization of octylmethacrylate and *N*-vinylimidazole with azobisisobutyronitrile, and used as a polymer-ligand (content of the vinylimidazolyl residue = 30 mol% ; $[\eta] = 0.64$ g/dl, toluene, 30°C by elemental analysis. viscometric measurement, respectively).

2.2.2 Spectroscopic Measurement

Distilled dichloromethane solutions of CoP and OIm were mixed together to obtain a CoP-OIm complex with mole ratio of $[\text{CoP}]:[\text{imidazolyl residue of OIm}] = 1:10$ ($[\text{CoP}] = 0.02 \text{ mmol l}^{-1}$).

Ultraviolet and visible absorption spectra of the CoP-OIm solution were measured in the temperature range from -15 - -30°C with UV spectrophotometer (JASCO V-550). At the low-temperature measurement, a dry gas was charged in the spectrophotometer to avoid frosting on the cell windows.

Laser Flash photolysis measurement was carried out with a pulse laser flash spectrophotometer equipped with a kinetic data processor (UNISOKU FR-2000). The laser flash was applied perpendicular to the light path of the spectrophotometer. The rapid absorption change was recorded with a contact-type photomultiplier to cancel the noise caused by scattered light.

A red-transparent membrane was obtained by casting the solution on a glass plate (1 × 2 cm) under a nitrogen atmosphere. The membrane was dried in vacuo overnight to remove the solvent completely.

2.3 Reversible Oxygen-Binding in Cooled Solution

The CoP and OIm complexes were soluble in organic solvents such as toluene, chloroform, and THF. Complexation of CoP with the imidazolyl residue of OIm or the 5-coordinated structure as presented in the chart was confirmed by an ESR signal ($g_{\parallel}=2.03$ and $g_{\perp}=2.00$) with an eight-line hyperfine splitting spectrum attributed to the nitrogen on the CoP's 5th site.

The dichloromethane solution of the CoP-OIm complex was cooled (e.g., at -15°C). The UV/visible absorption of CoTPP (and CoTDP, CoTTP)-OIm changed from the spectrum ($\lambda_{\text{max}}=412$ and 530 nm) attributed to deoxy CoP under a nitrogen atmosphere to the spectrum ($\lambda_{\text{max}}=429$ and 547 nm) attributed to oxy CoP ($\text{Co}/\text{O}_2=1/1$ adduct) immediately after exposure to oxygen (Figure 2-1). The deoxy-oxy spectral change was reversible in response to the oxygen partial pressure with isosbestic points at 420 and 535 nm. For the CoOEP-OIm complex, deoxy: $\lambda_{\text{max}}=392$ and 550 nm, oxy: $\lambda_{\text{max}}=413$, 528 and 561 nm, isosbestic points = 400 , 519 , 537 and 558 nm. The oxy (oxygen-binding) equilibrium curves obeyed Langmuir isotherms to give the oxygen-binding affinity p_{50} (oxygen partial pressure at which half of the CoP binds with oxygen).

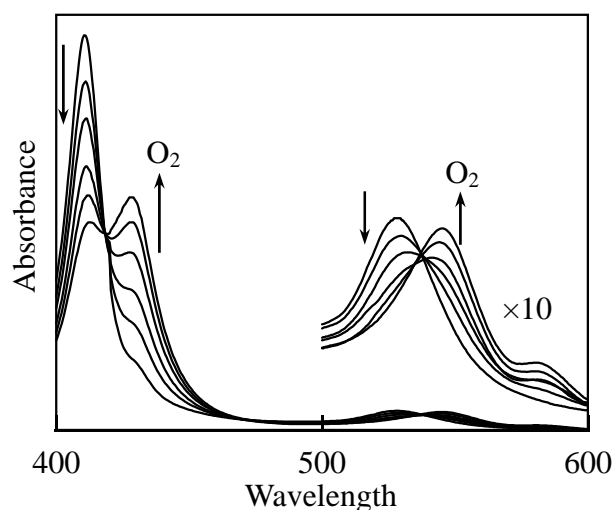


Figure 2-1. Visible absorption spectra of the CoTPP-OIm complex in CH_2Cl_2 at -15°C . O_2 partial pressure = 0, 15, 30, 46, 61, 76 cmHg.

2.4 Affinity and Kinetic Parameters

The oxygen-binding affinity p_{50} is listed in Table 2-1. The enthalpy and entropy changes (ΔH and ΔS) for the oxygen-binding were determined from the temperature dependence of the p_{50} and are also given in Table 2-1. ΔH or the enthalpy gain through the oxygen-binding for the polymeric CoP-OIm complexes was smaller than that for the corresponding monomeric CoP complex, which caused a slight decrease in the oxygen-binding affinity. p_{50} for the CoTPP complex of OIm [vinylimidazole residue content = 48mol%] was larger than that for the CoTPP-OIm [25mol%] complex. The affinity for the CoTDP and CoTTP complexes were lower than that for CoTPP. These results suggest a steric hindrance effect by the OIm polymer-ligand and CoP molecules.

Table 2-1. Oxygen-binding Affinity, Thermodynamic and Kinetic Parameters for the CoP-OIm Complexes in CH_2Cl_2 at -15°C : Imidazole residue content of OIm = 30mol%.

CoP	p_{50} [cmHg]	ΔH [kcal/mol]	ΔS [e.u.]	$10^{-8}k_{\text{on}}$ [$\text{M}^{-1}\text{s}^{-1}$]	$10^{-5}k_{\text{off}}$ [s^{-1}]
CoTPP ^{a)}	19	-14	-43	6.3	6.5
CoTPP ^{b)}	19	-11	-31		
CoTPP ^{c)}	27	-13	-39	2.0	2.2
CoTDP	28	-13	-48	1.8	3.7
CoTTP	33	-13	-50	1.5	3.9
CoOEP ^{a)}	21	-9.4	-35	0.7	0.8
CoOEP	17	-11	-43	0.2	0.5
CoTpivPP	2	-14	-28	2.9	0.2

^{a)} The CoP complex with *N*-benzylimidazole, Imidazolyl residue content of OIm = ^{b)}25 and ^{c)}48mol%, respectively

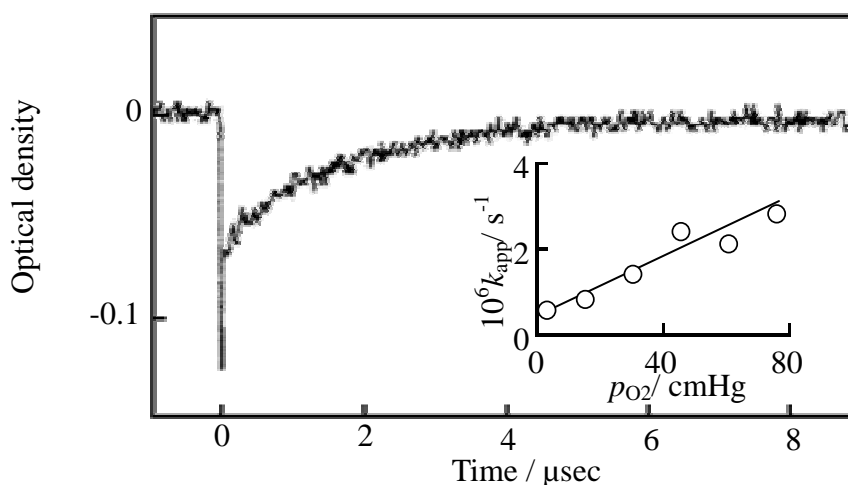


Figure 2-2. Absorbance change at 430nm after the laser irradiation for the CoTPP-OIm complex in CH_2Cl_2 at -15°C . Inset: Apparent oxygen-binding rate constant k_{app} vs partial oxygen pressure.

Photodissociation and recombination of the bound oxygen from and to the CoP complex in the cooled solution were monitored by laser flash photolysis. An example of the oxygen recombination time curve is shown in Figure 2-2. The reaction was completed within a few microseconds, and it was very rapid despite a reaction at low temperature. The oxygen-binding and -releasing rate constants (k_{on} and k_{off} in Eq. 2) were estimated by pseudo-first-order kinetics, as shown in the inset of Figure 2-2, and are also given in Table 1. The oxygen-releasing k_{off} values were on the order of 10^5 s^{-1} for the CoP complexes, and this significantly large k_{off} is the origin of the very low oxygen-binding affinity of the CoP complexes (or the reason why an oxygen adduct could be observed only at low temperature).

2.5 Extrapolation to Room Temperature

Figure 2-3 show the linear logarithmic p_{50} and k_{on} vs $1/T$ plots (van't Hoff and Arrhenius plots) and their extrapolations to 25°C . The extrapolated p_{50} , k_{on} , and k_{off} values at 25°C for the CoTPP-OIm complex are given in Table 2-2, with those for the typical oxygen carrier, CoTpivPP. The p_{50} value of 790 cmHg indicates a very weak oxygen-binding affinity of the CoP complex at 25°C (ca. 1/30 of the CoTpivPP's affinity), but suggests that an oxygen adduct could be observed for CoP under a high oxygen pressure, for example, 10 atm. The extrapolated k_{off} value was on the order of 10^8 s^{-1} for the CoP complex and more than 200 times larger than that of CoTpivPP, and it is concluded that this extremely large oxygen-releasing rate constant causes the very low oxygen-binding affinity.

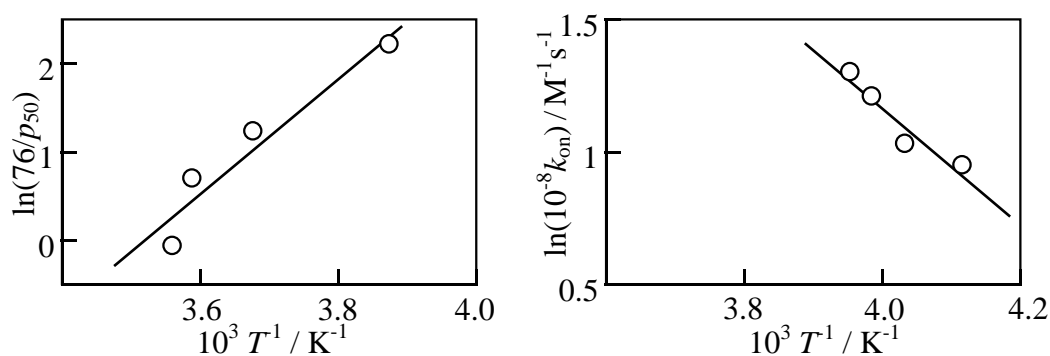


Figure 2-3. van't Hoff and Arrhenius plots of the oxygen-binding affinity p_{50} and rate constant k_{on} , respectively, for the CoTPP-OIm complex in CH_2Cl_2 .

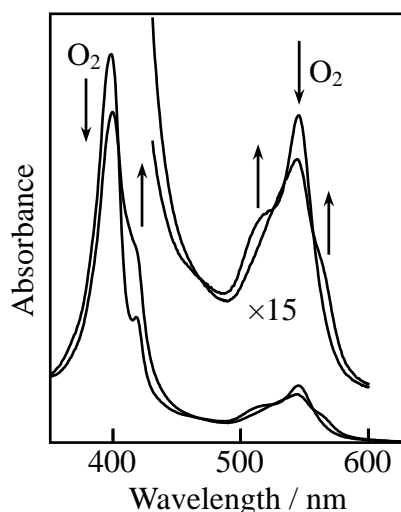
Table 2-2 Oxygen-binding Affinity and Binding and Releasing Rate Constants for the CoP-OIm and the CoTpivPP-OIm Complex at 25°C

Porphyrin	p_{50} / cmHg	$10^{-8} k_{\text{on}} / \text{M}^{-1} \text{s}^{-1}$	$10^{-5} k_{\text{off}} / \text{s}^{-1}$
CoTPP	790	13	1700
CoTpivPP	25	8.4	7.3
CoOEP	980	0.5	76

2.6 Reversible Oxygen-binding and Kinetics of the CoOEP-OIm membrane at low temperature.

Complexation of CoP such as the CoTPP to an imidazolyl residue of a polymer ligand yielded both an active and homogeneous dispersed CoTPP for oxygen-binding in solid state.

Both CoTPP and CoOEP have a simple and planar porphyrin structure, thus they have the similar value for the kinetic parameters such as oxygen-binding and -releasing rate constants. Compared with CoOEP, the deoxy-oxy spectral change of CoTPP membrane was not so clear, thus CoOEP was used for the spectroscopic measurement.

**Figure 2-4.** Visible absorption spectra of the CoOEP-OIm membrane at -20°C .

The red-colored membrane piece reversibly displayed a visible absorption spectrum ($\lambda_{\text{max}} = 392$ and 550 nm) attributed to deoxy CoTPP under a nitrogen atmosphere and the spectrum ($\lambda_{\text{max}} = 413$, 528 , and 561 nm oxy ($\text{Co}/\text{O}_2 = 1/1$ adduct) immediately after exposure to oxygen (shown in Figure 2-4). The deoxy-oxy spectral change was rapid and reversible in response to the oxygen partial pressure with isosbestic points at 400 ,

519, 537, and 558 nm. The oxygen-binding equilibrium curves obeyed Langmuir isotherms to give the oxygen-binding affinity p_{50} (oxygen partial pressure at which half of the CoTPP binds with oxygen) shown in Table 2-3. The recombination-time curve of oxygen on the CoOEP-OIm membrane at -15°C is given in Figure 2-5, which shows that the reaction was rapidly completed within a microsecond, despite a low temperature.

Changing the monitoring wavelength from 400 to 420 nm allowed the differential spectrum to be measured before and after the flash photolysis. The negative extreme in the differential spectrum, 413 nm, was selected as the monitoring wavelength. This wavelength agreed with the absorption maximum of the oxygen adduct in the UV region.

Table 2-3 Oxygen-binding affinity, thermodynamic and kinetic parameters for the CoP-OIm complexes at 25°C

Porphyrin	State ^{b)}	p_{50} cmHg	$10^{-5}k_{\text{on}}$ $\text{M}^{-1}\text{s}^{-1}$	$10^{-4}k_{\text{off}}$ s^{-1}
CoTPP ^{a)}	Soln	790	13000	17000
CoOEP ^{a)}	Membr	980	500	760
CoTpivPP	Membr	7.6	0.017	0.012

a) Extrapolated values from van't Hoff and Arrhenius plots of p_{50} , k_{on} , and k_{off} , respectively, at the temperature range of -35 - -15°C . b) Soln = CH_2Cl_2 solution, membr = the CoOEP-OIm solid membrane.

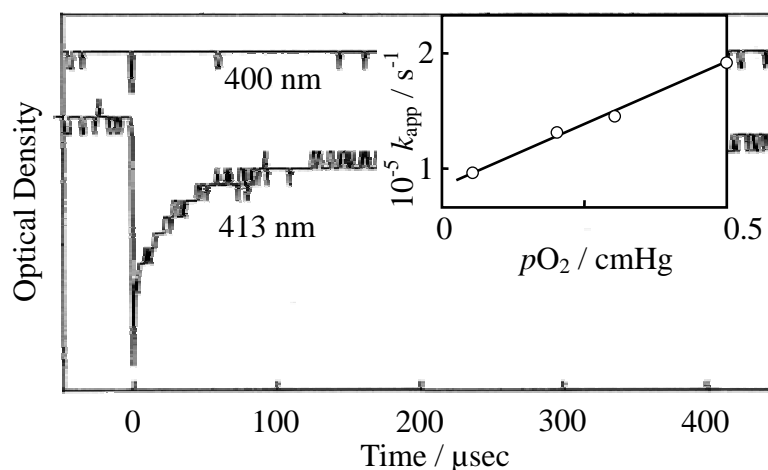


Figure 2-5. Recombination reaction of the photodissociated oxygen to the CoOEP complex of OIm in the solid membrane state. Spectral change after laser flash irradiation at -15°C . Inset: plots of apparent oxygen-binding rate constant (k_{app}) vs oxygen partial pressure ($p\text{O}_2$).

Plots of the apparent oxygen-binding rate constant k_{app} estimated from the time course of the absorbance change versus the oxygen partial pressure are shown in the inset in Figure 2-5. The linear relation indicates second-order kinetics for the oxygen binding to the cobaltporphyrin fixed in the polymer membrane. The oxygen-binding and oxygen-releasing rate constants, k_{on} and k_{off} , were calculated from the slope and intercept (as listed in Table 2-3).

2.7 Conclusion

Reversible oxygen-binding was observed at low temperature for the cobalt-tetraphenylporphyrin complex of poly(vinylimidazole-co-octylmethacrylate). Oxygen-binding affinity and rate constants were determined; low affinity for the tetraphenylporphyrin complex was attributed to enormously large oxygen-releasing rate constant. Solid membrane of the tetraphenylporphyrin complex also displayed the reversible oxygen-binding at low temperature.

These results suggest that the polymer-combined simple cobaltporphyrins would reversibly bind oxygen under a high oxygen pressure and are potentially applicable as an oxygen-permselective membrane.

References

1. J. P. Collman, *Acc. Chem. Res.* **1977**, *10*, 265.
2. E. Tsuchida, H. Nishide, *Top. Curr. Chem.* **1986**, *132*, 63.
3. M. Momenteau, C. A. Reed, *Chem. Rev.* **1994**, *94*, 659.
4. J. P. Collman, R. R. Gagne, C. A. Reed, T. R. Halbert, G. Lang, W. T. Robinson, *J. Am. Chem. Soc.* **1975**, *97*, 1427.
5. D. V. Stynes, H. C. Stynes, J. A. Ibers, B. R. James, *J. Am. Chem. Soc.* **1973**, *95*, 1142.
6. D. V. Stynes, H. C. Stynes, B. R. James, J. A. Ibers, *J. Am. Chem. Soc.* **1973**, *95*, 1796.
7. F. S. Molinaro, R. G. Little, J. A. Ibers, *J. Am. Chem. Soc.* **1977**, *99*, 5628.
8. H. Nishide, S. Hata, K. Mihayashi, E. Tsuchida, *Biopolymers* **1978**, *17*, 191.
9. E. Tsuchida, H. Nishide, *Adv. Polymer Sci.* **1977**, *24*, 1.
10. E. Tsuchida, T. Komatsu, E. Hasegawa, and H. Nishide; *J. Chem. Soc. Dalton. Trans.* 2713 (1990)